Molecular mechanism underlying ethanol activation of G-protein–gated inwardly rectifying potassium channels

Karthik Bodhinathan[a] and Paul A. Slesinger[a,b,1]

[a]Peptide Biology and Structural Biology Laboratories, The Salk Institute for Biological Studies, La Jolla, CA 92037; and [b]Department of Neuroscience, Icahn School of Medicine at Mount Sinai, New York, NY 10029

Edited by Lily Yeh Jan, University of California, San Francisco, CA, and approved October 1, 2013 (received for review June 17, 2013)

Alcohol (ethanol) produces a wide range of pharmacological effects on the nervous system through its actions on ion channels. The molecular mechanism underlying ethanol modulation of ion channels is poorly understood. Here we used a unique method of alcohol-tagging to demonstrate that alcohol activation of a G-protein–gated inwardly rectifying potassium (GIRK or Kir3) channel is mediated by a defined alcohol pocket through changes in affinity for the membrane phospholipid signaling molecule phosphatidylinositol 4,5-bisphosphate. Surprisingly, hydrophobicity and size, but not the canonical hydroxyl, were important determinants of alcohol-dependent activation. Altering levels of G protein Gβγ subunits, conversely, did not affect alcohol-dependent activation, suggesting a fundamental distinction between receptor and alcohol gating of GIRK channels. The chemical properties of the alcohol pocket revealed here might extend to other alcohol-sensitive proteins, revealing a unique protein microdomain for targeting alcohol-selective therapeutics in the treatment of alcoholism and addiction.

Kcnj6 | chemical modification | Kir3.2 | Dr-VSP | mPhosducin

Alcohol (ethanol) produces a wide range of pharmacological effects on the nervous system, ranging from anxiolytic effects to intoxication and alcohol addiction in certain individuals. Although the neural circuits underlying such addictive disorders are becoming better understood (1, 2), little is known about the molecular mechanisms underlying ethanol's interaction with specific target proteins, such as ion channels. G-protein–gated inwardly rectifying K^+(GIRK or Kir3) channels are activated by concentrations of ethanol relevant to human consumption (18 mM ethanol or 0.08% blood alcohol level) (3–5) and have been found to play a key role in alcohol-related disorders (6–9). For example, mice lacking GIRK2 (or Kir3.2) channels self-administer more ethanol and fail to develop conditioned place preference for ethanol, compared with wild-type (WT) littermates (6, 10). These results support a model in which ethanol may have lost its target in GIRK knockout mice, thus failing to elicit behaviors associated with ethanol consumption. Receptor activation of GIRK channels generates an outward, slow inhibitory postsynaptic current, which reduces neuronal activity (11). In addition to directly activating GIRKs, ethanol potentiates the slow inhibitory postsynaptic potential in midbrain dopamine neurons of the ventral tegmental area (8), which is produced by $GABA_B$ receptor activation of GIRK channels (7, 12, 13). Together these observations implicate GIRK channels in the etiology of alcohol dependence and addiction; however, the molecular details underlying ethanol activation of GIRK channels remain unknown.

A major challenge is to understand how ethanol, with its simple chemistry of only two carbons and a hydroxyl, can produce behavioral changes with rapidity and reproducibility. Ethanol has little volume or distinguishing stereochemistry. Although it was once thought to interact nonspecifically with membrane lipids, a preponderance of evidence suggests that ethanol binds directly to discrete pockets in proteins that alter their function (14, 15). However, unlike other typical drug interactions, ethanol has low potency (millimolar range) and lacks chemical specificity (more than one type of alcohol interacts with the same ion channel). Structural views of putative alcohol-binding pockets are emerging (3, 16, 17), but the molecular details and chemical rules governing the interaction of alcohol with these specific alcohol-binding pockets remain elusive.

In this study, we investigated the chemical nature of the alcohol pocket by expanding the method of "alcohol-tagging" ion channels (18). Using this unique strategy, we examined the chemical diversity of ligands compatible with the alcohol pocket and investigated the role of other signaling molecules, phosphatidylinositol 4,5-bisphosphate (PIP_2) (19, 20) and G-protein Gβγ subunits (21–24), which also regulate the activity of GIRK channels. Understanding this mechanism will be critical for developing alcohol-selective therapeutics that can perhaps prevent alcohol abuse and treat addiction.

Results

Alcohol Tagging the Intracellular Pocket Activates GIRK Channel. To elucidate the chemical rules governing alcohol activation of GIRK channels, we used a strategy of alcohol tagging the GIRK channel (18). We engineered GIRK2 (or Kir3.2) with a single thiol-reactive cysteine (Cys) at or near the alcohol pocket, a region comprising the βD–βE and βL–βM loops and N-terminal domain (Fig. 1*A*) (3). First, four native Cys residues in the cytoplasmic domain were replaced with thiol-unreactive residues to create a "Cys-less" GIRK2 (referred to as GIRK2*). GIRK2*

Significance

G-protein–gated inward-rectifying K^+ (GIRK) channels control neuronal excitability in the brain's reward circuit. Ethanol, a widely available drug of abuse, directly binds to a hydrophobic pocket in the GIRK channel and activates it. The molecular mechanism underlying ethanol activation of GIRK channel remained unknown. Here, we used specialized biophysical tools and discovered that ethanol associates directly with the GIRK channel, leading to enhanced interaction with a membrane phospholipid phosphatidylinositol 4,5-bisphosphate and activation of the channel. Most importantly, the alcohol-binding pocket in GIRK channels can be occupied by non-alcohol-like chemical groups that activate the channel. This study will enable the design of therapeutics to selectively block alcohol's access to GIRK channel.

Author contributions: K.B. and P.A.S. designed research; K.B. performed research; K.B. and P.A.S. contributed new reagents/analytic tools; K.B. and P.A.S. analyzed data; and K.B. and P.A.S. wrote the paper.

The authors declare no conflict of interest.

This article is a PNAS Direct Submission.

[1]To whom correspondence should be addressed. E-mail: paul.slesinger@mssm.edu.

This article contains supporting information online at www.pnas.org/lookup/suppl/doi:10.1073/pnas.1311406110/-/DCSupplemental.

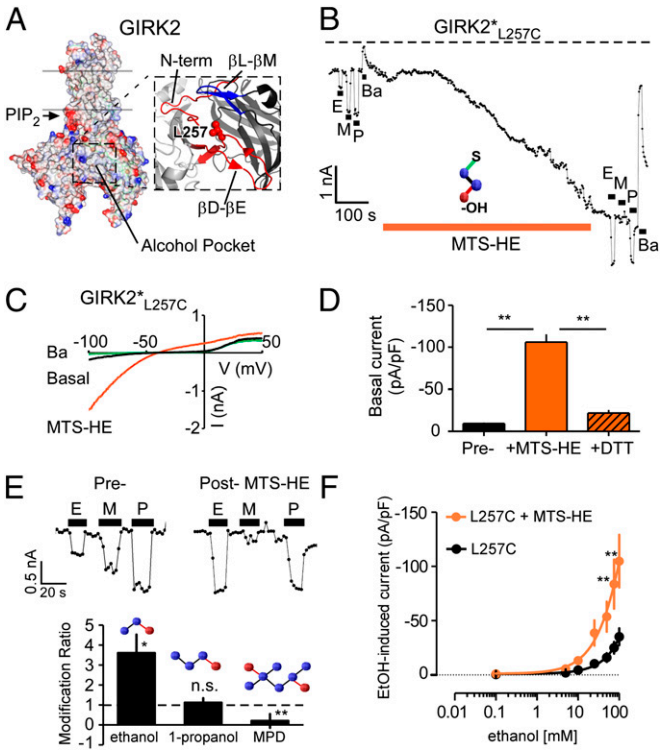

Fig. 1. Alcohol-tagging the pocket constitutively opens GIRK2 channels. (*A*) Crystal structure (3.6-Å resolution; adapted from ref. 25) of GIRK2 shows L257 (red) in the alcohol pocket, formed by part of N-terminal domain (N-term), βD–βE, and βL–βM loops from two adjacent subunits (blue and red). PIP_2 binds at the interface between transmembrane and cytosolic domains (arrow). (*B*) Plot of inward current through $GIRK2^*_{L257C}$ (at −100 mV) shows responses to ethanol (E), MPD (M), 1-propanol (P) (100 mM each), and Ba^{2+} (1 mM) before and after modification by 1 mM MTS-HE (orange bar). In this and subsequent figures, a dashed line represents zero current level. (*C*) Current–voltage plots show currents for $GIRK2^*_{L257C}$ recorded in extracellular 20K solution (containing 20 mM KCl, 140 mM NaCl, 0.5 mM $CaCl_2$, 2 mM $MgCl_2$, and 10 mM Hepes; pH 7.4, ∼318 mOsm) alone (basal, black), following exposure to 1 mM MTS-HE (orange) and then exposure to Ba^{2+} (green). (*D*) Ba^{2+}-sensitive basal $GIRK2^*_{L257C}$ current (pA/pF) before and after MTS-HE, and subsequent reversal by DTT (1 mM) ($n = 5$). $^{**}P < 0.01$. (*E*, *Upper*) Examples of $GIRK2^*_{L257C}$ current at −100 mV elicited by alcohols, before and after MTS-HE. (*Lower*) Bar graph shows MTS-HE modification ratio ($I_{induced}$ post/$I_{induced}$ pre-MTS) for ethanol ($n = 7$), 1-propanol ($n = 7$), and MPD ($n = 7$). $^*P < 0.05$; $^{**}P < 0.01$; n.s., not significant (paired Student *t* test). Dashed line indicates no effect of MTS-HE. (*F*) Dose–response curves for ethanol-induced current for $GIRK2^*_{L257C}$ (pA/pF) before ($n = 6$; black circles) and after ($n = 6$; orange circles) MTS-HE. Note the increase in amplitude of current following MTS-HE modification. $^{**}P < 0.01$ (repeated-measures ANOVA followed by Bonferroni's post hoc test).

channels retained normal activation by alcohol and G proteins (Table S1). We then introduced a single Cys at L257 in the βD–βE loop of GIRK2* and heterologously expressed $GIRK2^*_{L257C}$ in HEK293T (Fig. 1*A*). Hydroxyethyl methanethiosulfonate (MTS-HE) reagent induced an inward current through $GIRK2^*_{L257C}$ that reached a steady-state level within 600 s and persisted following removal of MTS-HE (Fig. 1*B*). By contrast, MTS-HE did not alter basal GIRK2* currents (Table S1). Notably, MTS-HE–activated $GIRK2^*_{L257C}$ currents strongly rectified like WT GIRK2 and were Ba^{2+}-sensitive (Fig. 1*C*). The reducing agent DTT reversed the MTS-HE–mediated increase in GIRK current, confirming the formation of a disulfide bond between $GIRK2^*_{L257C}$ and MTS-HE (Fig. 1*D*).

MTS-HE modification of $GIRK2^*_{L257C}$ also altered the rank order of alcohol activation, showing reduced activation by the bulkier alcohol, 2-methyl-2,4-pentanediol (MPD) (Fig. 1 *B* and *E*). MTS-HE modification may have altered the alcohol-pocket chemistry and size of the pocket, limiting access to MPD. Conversely, ethanol activation increased threefold following MTS-HE modification of $GIRK2^*_{L257C}$, suggesting that the hydrophobic pocket may be optimally occupied with MTS-HE and one or more ethanols (Fig. 1*E*). Comparison of dose–response curves for ethanol-induced currents before and after MTS-HE modification suggested that the potentiation resulted from an increase in efficacy (Fig. 1*F*). However, the inability to use saturating concentrations of ethanol precluded measuring the EC_{50} (3–5).

MTS-HE activation of $GIRK2^*_{L257C}$ developed slowly over 8–10 min, possibly due to membrane restricted diffusion. To test this hypothesis, we applied MTS-HE intracellularly (Fig. S1 *A* and *B*) and observed a concentration-dependent increase in the rate of MTS-HE activation, having a rate constant of 90.6 ± 17.2 $M^{-1}{\cdot}s^{-1}$ ($n = 11$) (Fig. S1 *C* and *D*). In summary, these findings provide evidence that alcohol tagging a single amino acid in the alcohol pocket can induce or support global changes that lead to GIRK channel opening.

Chemical Rules Governing Alcohol-Pocket Activation: Hydrophobicity and Size. To explore the chemical rules governing alcohol activation of GIRK, we compared the effects of tagging Cys in the pocket with MTS-E (ethyl), MTS-HE (hydroxyethyl), MTS-F

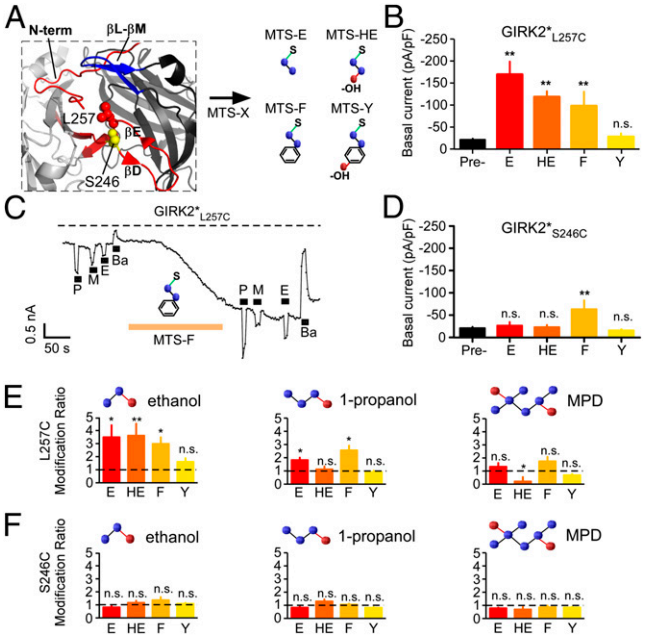

Fig. 2. Chemical diversity rules for activation mediated by the alcohol pocket. (*A*) Structural view of alcohol pocket in GIRK2 highlighting L257 (red) and S246 (yellow). Cys substitution forms disulfide bond with MTS reagent (MTS-X) carrying ethyl (MTS-E), hydroxyethyl (MTS-HE), benzyl (MTS-F), or hydroxybenzyl (MTS-Y) moieties. (*B*) Ba^{2+}-sensitive $GIRK2^*_{L257C}$ current (pA/pF) before (pre) and after modification by MTS-E (E; 0.1 mM), MTS-HE (HE; 1 mM), MTS-F (F; 0.01 mM), and MTS-Y (Y; 0.1 mM). All MTS reagents except MTS-Y showed significant increase in basal current. $^{**}P < 0.01$; n.s., not significant. (*C*) Plot shows inward $GIRK2^*_{L257C}$ current (at −100 mV) and responses to 1-propanol (P), MPD (M), ethanol (E) (100 mM each), and 1 mM Ba^{2+} before and after modification by MTS-F (0.01 mM; light orange bar). (*D*) Ba^{2+}-sensitive $GIRK2^*_{S246c}$ current (pA/pF) before (pre) and after modification with the indicated MTS reagent. All MTS reagents except MTS-F showed no significant change in current. $^{**}P < 0.01$; n.s., not significant. (*E* and *F*) Modification ratio profiles for $GIRK2^*_{L257C}$ (*E*) and $GIRK2^*_{S246C}$ (*F*) for ethanol (*Left*), 1-propanol (*Center*), and MPD (*Right*), after modification by the indicated MTS reagent. $^*P < 0.05$; $^{**}P < 0.01$; n.s., not significant (paired Student *t* test).

(benzyl or phenylalanine-like), or MTS-Y (hydroxy-benzyl or tyrosine-like) (Fig. 2*A*). Both MTS-E (0.1 mM) and MTS-F (0.01 mM) significantly increased GIRK2$^*_{L257C}$ currents, reaching a steady-state level similar to that of MTS-HE (Fig. 2 *B* and *C*). Thus, ethyl and benzyl moieties can also be accommodated in the pocket, similar to hydroxyethyl. However, MTS-Y (0.1 mM) did not alter basal GIRK2$^*_{L257C}$ currents (MTS-Y alone, −27.4 ± 8.3 pA/pF; $n = 5$). To determine whether MTS-Y chemically reacted with GIRK2$^*_{L257C}$, we applied MTS-HE following exposure to MTS-Y and did not observe a MTS-HE–dependent increase in current [MTS-HE alone, −118.2 ± 13.3 pA/pF ($n = 7$) vs. MTS-HE after MTS-Y, −28.3 ± 4.2 pA/pF ($n = 5$)]. This result suggests that, although MTS-Y tags GIRK2$^*_{L257C}$, minor increases in side-chain volume and hydrophilicity with the additional hydroxyl (MTS-Y vs. MTS-F) prevent its access to the hydrophobic pocket. To explore the physical constraints on access to the pocket, we introduced a Cys at S246; in the GIRK2 crystal structure (25), S246 is in the same βD–βE loop ∼6–7 Å away from L257 and farther from the pocket (Fig. 2*A*). Similar to GIRK2$^*_{L257C}$, application of MTS-Y (0.1 mM) for 8–10 min did not alter basal GIRK2$^*_{S246C}$ currents (Fig. 2*D*). Notably, neither MTS-E (0.1 mM) nor MTS-HE (1 mM) altered basal GIRK2$^*_{S246C}$ current, consistent with the short side chains of these compounds failing to reach the pocket. However, MTS-F (0.01 mM) slightly increased basal GIRK2$^*_{S246C}$ current (Fig. 2*D*), indicating that S246C can be modified, and that the benzyl, but not the hydroxyl-benzyl, moiety can engage the alcohol pocket, similar to L257C.

Comparison of the amplitude of alcohol-induced currents before and after MTS modification (modification ratio) can reveal changes in pocket volume and accessibility. Interestingly, MTS-E, -HE, and -F significantly enhanced the ethanol modification ratio in GIRK2$^*_{L257C}$ (Fig. 2*E*). The modification ratio for MPD-activated currents, however, was unchanged or smaller (Fig. 2*E*), indicating steric hindrance to larger alcohols. In sharp contrast, MTS reagents did not alter the modification ratio for ethanol, MPD, or 1-propanol for GIRK2$^*_{S246C}$ (Fig. 2*F*). Together, these results suggest that MTS reagents that are situated within the alcohol pocket (L257), but not near it (S246), can enhance ethanol but not MPD activation.

Altering Levels of Receptor-Derived Gβγ Subunits Does Not Affect MTS-HE–Activated GIRK Channels. G-protein Gβγ subunits, part of the heterotrimeric Gαβγ G protein complex, are released upon stimulation of the Gα$_{i/o}$ family of G-protein–coupled receptors and directly activate GIRK channels (21–24, 26). Therefore, the MTS-dependent activation of GIRK2$^*_{L257C}$ could result from chemical enhancement of Gβγ interaction. To investigate this possibility, we examined MTS-HE activation with either overexpressed myristoylated phosducin (mPhos) to chelate free Gβγ (27) or overexpressed Gβ1 and Gγ2 subunits to increase basal Gβγ levels (Fig. 3*A*). Confirming previous findings with GIRK channels (27), Gβγ overexpression increased basal GIRK2* currents (Fig. S2 *A* and *B*), and mPhos expression reduced receptor-activated currents (Fig. S2 *A* and *C*). By contrast, mPhos did not alter the rate of activation or steady level of current with MTS-HE–treated GIRK2$^*_{L257C}$ (Fig. 3 *B* and *C*). Moreover, overexpression of Gβγ also did not alter the rate (Fig. 3*C*) or amplitude (Fig. 3*D*) of MTS-HE–activated GIRK2$^*_{L257C}$ currents. These results suggest that activation of GIRK channels via chemical modification of the alcohol pocket does not require direct association with Gβγ subunits.

To probe this model further, we investigated the effect of alcohol-tagging L344, a key Gβγ interaction site, located in the βL–βM loop (∼11–13 Å away from L257 and the alcohol pocket; refs. 28–30) (Fig. 4*A*). Indeed, previous work suggested an interaction between Gβγ and modulation of GIRKs with halothane (31), raising the possibility of an interaction between alcohol activation and Gβγ-binding sites. Interestingly, before MTS

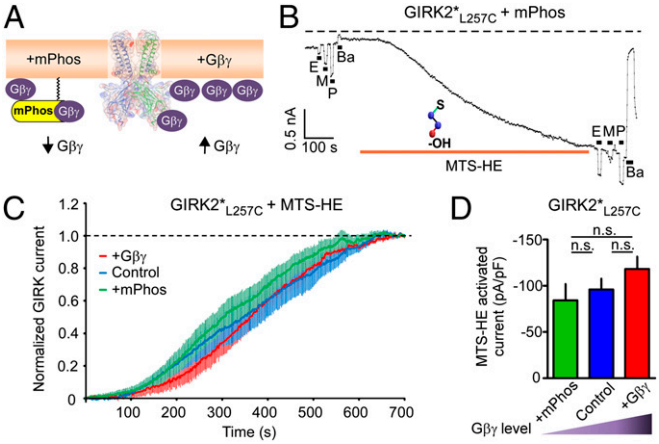

Fig. 3. MTS-HE activation of GIRK2$^*_{L257C}$ channels is independent of Gβγ G proteins. (*A*) Schematic depicts method for reducing Gβγ (expression of mPhos, +mPhos) or increasing Gβγ (expression of Gβ$_1$γ$_2$, +Gβγ). (*B*) Plot of inward current through GIRK2$^*_{L257C}$ channels (at −100 mV) in HEK293T cells coexpressing mPhos shows alcohol responses and MTS-HE induction. (*C*) Time course of MTS-HE–dependent activation of GIRK2$^*_{L257C}$ currents (normalized current ±SEM vs. time) under reduced (+mPhos; green line), basal (control; blue line), and increased (+Gβγ; red line) levels of Gβγ. (*D*) Bar graph shows MTS-HE–activated currents for GIRK2$^*_{L257C}$ (pA/pF) with +mPhos ($n = 5$), basal ($n = 8$), and +Gβγ ($n = 7$). There was no statistical difference in the amplitude of MTS-HE–activated currents with different levels of Gβγ. n.s., not significant.

modification, GIRK2$^*_{L344C}$ exhibited large, agonist-independent basal currents that were sensitive to Gβγ chelation by mPhos, suggesting enhanced Gβγ interaction with GIRK2$^*_{L344C}$ (Fig. 4*E*). In contrast to GIRK2$^*_{L257C}$, however, MTS-HE inhibited the large basal GIRK2$^*_{L344C}$ current (Fig. 4*B*), leaving a small, inwardly rectifying current (Fig. 4 *B* and *C*) that exhibited a normal rank order of alcohol activation (compare with Fig. 1*E*). Interestingly, MPD-activated currents for unmodified GIRK2$^*_{L344C}$ were smaller than ethanol-activated and 1-propanol–activated currents (Fig. S3), raising the possibility that access of bulkier alcohols to the pocket is partially restricted by increased binding of Gβγ to L344C. As expected, modulating levels of Gβγ altered the kinetics of MTS-HE–mediated inhibition of GIRK2$^*_{L344C}$, where the rate of inhibition was significantly faster (T_{50}, 21.4 ± 2.1 s; $n = 7$) with reduced Gβγ (+mPhos) and slower (58.7 ± 10.3 s; $n = 6$) with elevated Gβγ (+Gβγ), compared with control (38.1 ± 2.6 s; $n = 14$) ($P < 0.05$; ANOVA followed by Bonferroni's multiple comparison post hoc test; Fig. 4*D*). The extent of MTS-HE–dependent inhibition of GIRK2$^*_{L344C}$ current was similar between all three groups (Fig. 4*E*), indicating that Gβγ levels modulate the rate, but not the amplitude, of MTS-HE inhibition. Together, these results suggest that, although alcohol activation is insensitive to Gβγ levels, these two activators seem to share a common pathway that is independently engaged, via conformational changes in the cytoplasmic domains around the pocket that are relayed to transmembrane gates.

Alcohol Activation Increases Relative Affinity of PIP$_2$–GIRK Interaction. PIP$_2$ association with GIRK was shown to be essential for Gβγ activation (19, 20). However, it was unknown whether alcohol activation also required channel interactions with PIP$_2$. To test for PIP$_2$ dependence, we expressed a voltage-sensing phosphatase from zebrafish *Danio rerio* (Dr-VSP), which removes the 5′ phosphate of PIP$_2$ and thereby depletes levels of membrane-bound PIP$_2$ (32). A 500-ms depolarizing pulse to +100 mV activates Dr-VSP (Fig. 5*A*), leading to rapid inhibition of GIRK2* current at −100 mV (25). We first examined whether MTS-dependent activation of GIRK2$^*_{L257C}$ is dependent on PIP$_2$. Activation of Dr-VSP

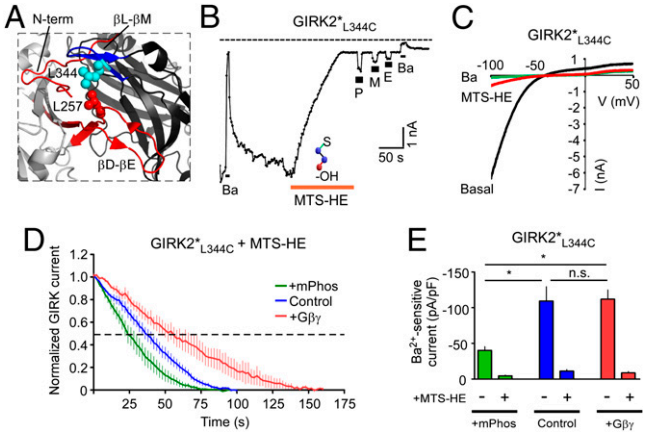

Fig. 4. Alcohol tagging inhibits GIRK2*$_{L344C}$ in a G-protein–dependent manner. (*A*) Structural view of alcohol pocket in GIRK2 highlighting L344 (cyan) in the βL–βM loop, part of the Gβγ binding site (11). (*B*) Plot of inward current through GIRK2*$_{L344C}$ (at −100 mV) shows inhibition of large basal current with MTS-HE (1 mM). Note the WT-like alcohol activation (rank order: P>M>E) after MTS-HE modification. (*C*) Current–voltage plots show currents for GIRK2*$_{L344C}$ recorded in extracellular 20K solution alone (basal; black), following exposure to 1 mM MTS-HE (red) and then exposure to 1 mM Ba^{2+} (green). The large, inwardly rectifying basal GIRK2*$_{L344C}$ current is inhibited by MTS-HE and is also Ba^{2+}-sensitive. (*D*) Time course of MTS-HE–dependent inhibition of GIRK2*$_{L344C}$ (normalized current ±SEM vs. time) under reduced (+mPhos; $n = 7$), basal (control; $n = 14$), and increased (+Gβγ; $n = 6$) levels of Gβγ. Rate of MTS-HE–dependent inhibition increases with lower Gβγ levels. (*E*) Ba^{2+}-sensitive GIRK2*$_{L344C}$ current for +mPhos ($n = 7$), basal ($n = 14$), and +Gβγ ($n = 6$) in the absence and then presence of MTS-HE (1 mM). In the unmodified state (–), +mPhos (−40.2 ± 5.3 pA/pF, $n = 9$) significantly decreased basal GIRK2*$_{L344C}$ currents, compared with control (−109.3 ± 20.1 pA/pF, $n = 13$) and +Gβγ (−112.1 ± 12.9 pA/pF, $n = 6$). *$P < 0.05$; n.s., not significant. The extent of inhibition was indistinguishable for all three conditions ($P > 0.05$).

completely reversed the MTS-HE–activated GIRK2*$_{L257C}$ current (Fig. 5*B* and Fig. S4*A*). Importantly, the rank order of alcohol activation was preserved after activation of Dr-VSP (Fig. S4*B*), indicating little change in the alcohol pocket but significantly fewer active channels. Thus, MTS-activated GIRK channels require membrane-bound PIP_2.

To explore relative changes in GIRK affinity for PIP_2 following MTS modification, we varied the duration of activating pulse for Dr-VSP to tightly control the extent of PIP_2 depletion (33). The rate of current (τ) inhibition provides a measure of the relative affinity for PIP_2 (19, 20, 34), with a slower decay indicating an increase in PIP_2–GIRK affinity (19, 20, 32, 35). Dr-VSP–dependent inhibition of GIRK2*$_{L257C}$ current was markedly slower following MTS-HE modification (Fig. 5*C*). The τ increased in GIRK2*$_{L257C}$ channels activated with MTS-HE at all Dr-VSP depolarizations (Fig. 5*D*). We then investigated the possibility that MTS-HE treatment alone affected the function of Dr-VSP; there was no significant change in the rate of Dr-VSP–dependent inhibition after MTS-HE exposure (Fig. S5). Together, these results indicate that alcohol tagging the hydrophobic alcohol pocket in GIRK channels increases the relative affinity for PIP_2, leading to an increase in open channel probability (4).

Lastly, we examined whether alcohol-dependent activation of WT GIRK2 channels also increases the relative affinity for PIP_2. We coexpressed m2 muscarinic receptor with GIRK2* and Dr-VSP and measured the alcohol- and carbachol-induced currents before and after Dr-VSP activation (Fig. 6 *A* and *B*). Both alcohol- and carbachol-induced currents were significantly reduced following PIP_2 depletion. Similar to MTS-HE–modified GIRK2*$_{L257C}$ channels, GIRK2 channels that were preactivated with either 1-propanol or ethanol exhibited markedly slower rates of Dr-VSP–dependent inhibition (Fig. 6 *C* and *D*). To rule out possible hysteresis with two consecutive Dr-VSP activation protocols, we reproduced the experiment in the absence of alcohol; τ decreased slightly with the second Dr-VSP activation pulse, the opposite of our finding in the presence of alcohol (Fig. 6*E*). Thus, either alcohol tagging (MTS-HE) or alcohol (ethanol or 1-propanol) activation of GIRK channels slows PIP_2 depletion, suggesting that enhancement of the relative affinity for PIP_2 underlies an increase in open channel probability.

Discussion

Alcohol modulation of GIRK channels regulates neuronal excitability in the brain's reward circuit (11) and underlies forms of alcohol addiction (6, 8–10, 36). Here, we uncovered previously undescribed principles governing alcohol modulation of GIRK channels. Importantly, the canonical hydroxyl of alcohol was not essential for chemical-dependent activation of GIRK. Moreover, alcohol activation absolutely requires the membrane phospholipid signaling molecule PIP_2 but not the receptor-activated G protein Gβγ subunits. The chemical rules of hydrophobicity and size have significant implications for the development of chemical therapeutics that could occupy the pocket and block access to alcohol, revealing a unique strategy for treating alcohol abuse and addiction.

Chemical Nature of GIRK Alcohol Pocket. Alcohol-tagging a single residue located within (L257C), but not near (S246C), the alcohol pocket of GIRK channels leads to constitutive activation. Mascia et al. (18) used a similar approach of tagging $GABA_A$/glycine receptors and found that propyl-MTS (PMTS) could mimic some of the effects of anesthetics as well as occlude alcohol-dependent modulation. There are two significant differences worth highlighting. First, PMTS-dependent potentiation of $GABA_A$/glycine receptors was only evident with a low concentration of agonist and did not change maximal activation (18), whereas MTS-HE directly activated GIRKs with little dependence

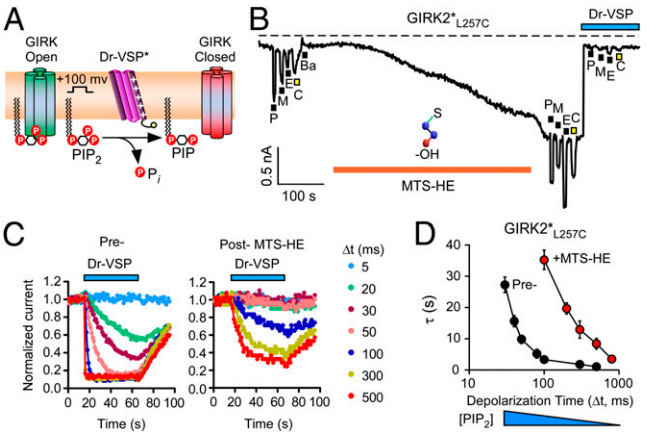

Fig. 5. MTS-HE activation of GIRK2*$_{L257C}$ is PIP_2-dependent. (*A*) Schematic shows method for reducing membrane-bound PIP_2. Voltage-dependent activation of Dr-VSP (+100 mV) activates the phosphatase, which converts PIP_2 to PIP, thus moving GIRK from PIP_2-bound open state (green) to unbound closed state (red). (*B*) Plot of inward current through GIRK2*$_{L257C}$ (at −100 mV) shows MTS-HE–dependent activation and then inhibition following Dr-VSP activation (blue bar). (*C*) Time course of inhibition for GIRK2*$_{L257C}$ (plot of normalized current vs. time) with variable intervals of Dr-VSP activation (Δt = 5, 20, 30, 50, 100, 300, and 500 ms) before (*Left*) and after (*Right*) MTS-HE modification. (*D*) Plot of time constant (τ) for Dr-VSP–dependent inhibition of GIRK2*$_{L257C}$ vs. depolarization time (longer time corresponds to lower PIP_2 levels). Note τ is smaller (indicating faster current decay) for longer depolarization times and is shifted to the right for MTS-HE–modified GIRK2*$_{L257C}$, suggesting increase in relative PIP_2 affinity for the modified channel.

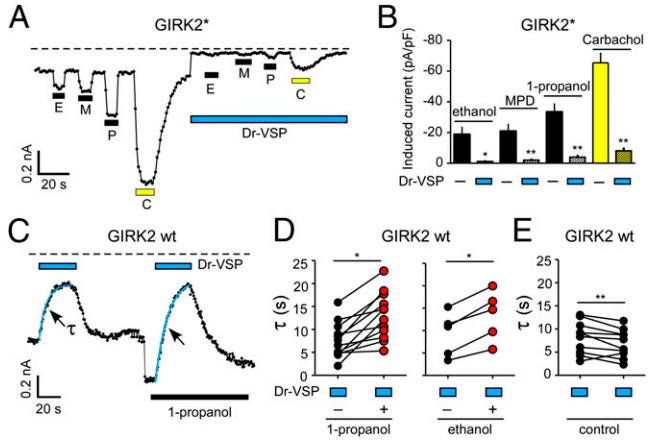

Fig. 6. Alcohol-activated GIRK2 channels exhibit higher relative affinity for PIP_2. (*A*) Plot of inward current through GIRK2* (at −100 mV) shows responses to ethanol (E), MPD (M), 1-propanol (P) (100 mM each), and carbachol (C, 5 μM) before and during activation of Dr-VSP (blue bar). PIP_2 depletion decreases both alcohol and carbachol-activated currents. m2 muscarinic receptor was coexpressed with GIRK2*. (*B*) Bar graph shows amplitude of induced currents for GIRK2* (pA/pF) with ethanol, MPD, 1-propanol ($n = 7$ each; 100 mM), and carbachol ($n = 5$; 5 μM) in the absence (–) and then presence (blue bar) of activated Dr-VSP. $*P < 0.05$; $**P < 0.01$ (paired Student *t* test). (*C*) Plot of inward current through WT GIRK2 channels (at −100 mV) shows transient inhibition with Dr-VSP activation ($\Delta t = 30$ ms) in the absence and then presence of 1-propanol (100 mM). A single exponential was fitted to current decay (τ, blue line). (*D*) Paired measurements of τ for GIRK2 WT in the absence (black circles) and presence (red circles) of 1-propanol (*Left*) or ethanol (*Right*). Note that τ is markedly larger in the presence of 1-propanol ($n = 12$ paired recordings) or ethanol ($n = 5$ paired recordings), suggesting increase in relative PIP_2 affinity; $*P < 0.05$ (paired Student *t* test). (*E*) Control experiment shows small decrease in τ with two consecutive Dr-VSP activation pulses ($n = 10$ paired recordings). $**P < 0.05$ (paired Student *t* test).

on Gβγ subunits. Second, PMTS modification blocked further modulation by alcohol (18), whereas MTS-HE modification of GIRKs mimicked alcohol and enhanced ethanol activation. Strikingly, MTS-E and -F, which lack hydroxyl moieties, were equally effective as MTS-HE at activating L257C channels. One interpretation is that the hydroxyl is not required for chemical-dependent activation but is essential for stabilizing native alcohols through hydrogen bonding (3). Formation of the disulfide bond alone, however, was insufficient for channel activation because MTS-Y modified L257C but did not activate the channel. The structural features and chemical forces observed for GIRK channels might apply to other alcohol pockets (37), such as with pentameric ligand-gated ion channels (16) and transient receptor potential channels (38). Recently, Sauguet et al. (39) examined the structural basis of potentiation by alcohols and anesthetics in an ethanol-sensitized prokaryotic channel; they describe an intersubunit hydrophobic pocket in which 2-bromoethanol forms both polar (hydrogen bonds) and nonpolar interactions with the channel, the same basic elements observed in GIRK channels.

MTS modification led to potentiation of ethanol-induced $GIRK2^*_{L257C}$ currents. One possible explanation is that the MTS reagent did not tag all four Cys residues (in each pocket), leaving one empty pocket for ethanol. Alternatively, the MTS-HE–tagged pocket may accommodate smaller alcohols like ethanol, but not larger alcohols like MPD. Consistent with this interpretation, ethanol, but not MPD, activated $GIRK2^*_{L257C}$ further after MTS-HE modification. Could the pocket accommodate two or more ethanol-like chemical compounds? We showed previously that MPD (212 $Å^3$) failed to activate GIRK channels when the native leucine (~101 $Å^3$) was replaced with tryptophan (168 $Å^3$), suggesting an optimal working volume of ~312 $Å^3$ (volume of Leu side-chain + MPD) (3). With MTS-HE–tagged $GIRK2^*_{L257C}$ channels, we found that ethanol and 1-propanol, but not MPD, activate the channel. If we consider that the thiol-hydroxyethyl in MTS-HE is ~116 $Å^3$ and the Cys side chain is ~50 $Å^3$, and assuming a volume of 96.9 $Å^3$ for ethanol and 124.3 $Å^3$ for 1-propanol, we calculate occupancy volumes of 262.9 $Å^3$ for ethanol, 290.3 $Å^3$ for 1-propanol, and 378 $Å^3$ for MPD. Thus, two alcohols could occupy the pocket—ethanol and hydroxyethyl or 1-propanol and hydroxyethyl. MPD, conversely, is unable to activate the MTS-modified channel due to its larger size (working volume > 312 $Å^3$). These results highlight the chemical nature and volumetric parameters of the alcohol pocket that make it a critical activation site for GIRK. Future investigations with atomic-resolution structures of GIRK alcohol pocket in complex with ethanol would improve our understanding of stoichiometry and spatial accommodation of individual alcohols and determine the stoichiometry of ethanol in the GIRK pocket.

Structural Model Underlying Alcohol-Dependent Activation. Previously, it was unclear whether alcohol interacts with GIRK activators like G-protein Gβγ subunits (21–24), Na^+ (40–43), ATP (19, 43, 44), and PIP_2 (19, 20, 45). Here, we show that Dr-VSP–mediated depletion of PIP_2 completely reversed MTS-activated and alcohol-induced GIRK currents, suggesting that alcohol activation of GIRK require PIP_2. Importantly, alcohol or MTS reagents did not affect PIP_2 or PIP kinase (enzyme that converts PIP to PIP_2) (46), because MTS reagents did not affect PIP_2-dependent basal current in GIRK2* or PIP_2 interaction with inward rectifiers (47). The reliance of Gβγ-activated (19, 20) and ethanol-activated GIRK channels on PIP_2 suggests convergence of gating mechanisms at the PIP_2 binding site.

By simultaneously interrogating PIP_2 binding affinity and channel opening with Dr-VSP, we found that both ethanol and MTS-HE slowed the rate of current decay produced by Dr-VSP activation. These results suggest that MTS activation and ethanol-dependent activation increase relative PIP_2–GIRK affinity. Similarly, presence of Gβγ slows the rate of current decay by anti-PIP_2 antibodies (19), indicating an increase in relative affinity. Accordingly, Dr-VSP–dependent inhibition was slower for L344C [31.0 ± 2.5 s ($n = 7$) vs. 6.2 ± 1.6 s ($n = 6$) for GIRK2*], a mutant with a large, agonist-independent basal current. Thus, alcohol-induced changes in affinity of GIRK for PIP_2 may recapitulate some of the same events induced by Gβγ binding. The cross-talk between alcohol, Gβγ, and the low affinity for PIP_2 suggest that GIRK channels have evolved to be sensitive to small molecules that either inhibit (48, 49) or activate (3–5) the channel.

Our findings support an "allosteric model," whereby increasing pocket hydrophobicity by chemical tagging or by alcohol itself lowers the free energy barrier (ΔG) for channel opening. Alcohol binds to the pocket, and produces weak van der Waals and hydrogen-bond interactions with residues in βD–βE and βL–βM loops that line the pocket, subsequently increasing PIP_2–GIRK affinity and leading to an increase in the probability of channel opening (NP_o). These conformational changes culminate in the movement of the channel's G loop and transmembrane gates (25, 34), permitting ion permeation. This model is compatible with features of GIRK alcohol pocket such as low affinity, low binding energy, and lack of chemical specificity for alcohols (14).

Receptor-dependent Gβγ activation, however, relies on direct protein–protein interaction between GIRKs and G proteins (21, 28–30). Previous reports suggested a difference in alcohol and receptor activation mechanisms (4, 5). In support of this finding, the rate of MTS-HE–dependent inhibition of basal currents in L344C, part of the Gβγ binding site in the βL–βM loop (28–30), was dependent on Gβγ levels, whereas MTS-HE activation of L257C channels was unaffected by varying Gβγ levels. However, alcohol-dependent (this study), Gβγ-dependent (19), and Na^{+z}-dependent (25, 40–42) activation all involve changes in PIP_2–GIRK affinity, suggesting a convergence of

these distinct activators at the PIP_2 binding site. The proximity of alcohol pocket and Gβγ binding site, which both involve the βL–βM loop previously implicated in GIRK activation (3, 25), may explain the partial overlap in these activation pathways. Possibly, Gβγ induces a conformational wave, similar to that in ligand-gated ion channels (50), which propagates to the PIP_2 binding site through the alcohol pocket.

After submission of our study, Whorton and MacKinnon described the high-resolution structure of Gβγ in complex with GIRK2 (51). The overlap between the Gβγ sites of interaction and the alcohol pocket is striking (Fig. S6). Leu55 on Gβ forms hydrogen bonds with L344 and several sites in the alcohol pocket (F254, P256, L342, and Y349) identified previously (3). Interestingly, L257 does not appear to be close enough to interact with Gβ. This arrangement raises the intriguing possibility that L55 activates GIRK channels by engaging the alcohol pocket, similar to how MTS modification of L257C may activate the channel.

Materials and Methods

SI Materials and Methods describes materials, mutagenesis, protocols for cell culture, whole-cell patch-clamp electrophysiology, Dr-VSP activation, and statistical analyses. Briefly, mutant or wild-type GIRK channels were expressed in HEK-293T cells and assessed for reactivity with MTS reagents. Modified channels were then tested for alcohol response and sensitivity to PIP_2 depletion.

ACKNOWLEDGMENTS. We thank Dr. Prafulla Aryal (Oxford University) for creating some GIRK mutants; Dr. Michael Pusch (Istituto di Biofisica) for comments on the manuscript; Dr. Yasushi Okamura (Osaka University) for Dr-VSP DNA; Dr. Nathan Dascal (Tel Aviv University) for m-Phos; Dr. Ian Glaaser (P.A.S. laboratory) for generating the Pymol figures; and Dr. Mark Shapiro (University of Texas Health Science Center, San Antonio) for discussion about Dr-VSP. We acknowledge technical assistance and support of the P.A.S. laboratory and Dr. Senyon Choe. This work was supported by American Heart Association Postdoctoral Fellowship 12POST9830002 (to K.B.); the 2011 Pioneer Fund Postdoctoral Scholarship (to K.B.); and National Institute on Alcohol Abuse and Alcoholism Grant AA018734 (to P.A.S.) and National Institute on Drug Abuse Grant DA019022 (to P.A.S.).

1. Koob GF, Volkow ND (2010) Neurocircuitry of addiction. *Neuropsychopharmacology* 35(1):217–238.
2. Hyman SE, Malenka RC, Nestler EJ (2006) Neural mechanisms of addiction: The role of reward-related learning and memory. *Annu Rev Neurosci* 29:565–598.
3. Aryal P, Dvir H, Choe S, Slesinger PA (2009) A discrete alcohol pocket involved in GIRK channel activation. *Nat Neurosci* 12(8):988–995.
4. Kobayashi T, et al. (1999) Ethanol opens G-protein-activated inwardly rectifying K^+ channels. *Nat Neurosci* 2(12):1091–1097.
5. Lewohl JM, et al. (1999) G-protein-coupled inwardly rectifying potassium channels are targets of alcohol action. *Nat Neurosci* 2(12):1084–1090.
6. Blednov YA, Stoffel M, Chang SR, Harris RA (2001) Potassium channels as targets for ethanol: Studies of G-protein-coupled inwardly rectifying potassium channel 2 (GIRK2) null mutant mice. *J Pharmacol Exp Ther* 298(2):521–530.
7. Cruz HG, et al. (2004) Bi-directional effects of GABA(B) receptor agonists on the mesolimbic dopamine system. *Nat Neurosci* 7(2):153–159.
8. Federici M, Nisticò R, Giustizieri M, Bernardi G, Mercuri NB (2009) Ethanol enhances GABAB-mediated inhibitory postsynaptic transmission on rat midbrain dopaminergic neurons by facilitating GIRK currents. *Eur J Neurosci* 29(7):1369–1377.
9. Kozell LB, Walter NA, Milner LC, Wickman K, Buck KJ (2009) Mapping a barbiturate withdrawal locus to a 0.44 Mb interval and analysis of a novel null mutant identify a role for Kcnj9 (GIRK3) in withdrawal from pentobarbital, zolpidem, and ethanol. *J Neurosci* 29(37):11662–11673.
10. Hill KG, Alva H, Blednov YA, Cunningham CL (2003) Reduced ethanol-induced conditioned taste aversion and conditioned place preference in GIRK2 null mutant mice. *Psychopharmacology (Berl)* 169(1):108–114.
11. Lüscher C, Slesinger PA (2010) Emerging roles for G protein-gated inwardly rectifying potassium (GIRK) channels in health and disease. *Nat Rev Neurosci* 11(5):301–315.
12. Padgett CL, et al. (2012) Methamphetamine-evoked depression of GABA(B) receptor signaling in GABA neurons of the VTA. *Neuron* 73(5):978–989.
13. Arora D, et al. (2011) Acute cocaine exposure weakens GABA(B) receptor-dependent G-protein-gated inwardly rectifying K^+ signaling in dopamine neurons of the ventral tegmental area. *J Neurosci* 31(34):12251–12257.
14. Harris RA, Trudell JR, Mihic SJ (2008) Ethanol's molecular targets. *Sci Signal* 1(28):re7.
15. Hansen SB, Tao X, MacKinnon R (2011) Structural basis of PIP_2 activation of the classical inward rectifier K^+ channel Kir2.2. *Nature* 477(7365):495–498.
16. Howard RJ, et al. (2011) Structural basis for alcohol modulation of a pentameric ligand-gated ion channel. *Proc Natl Acad Sci USA* 108(29):12149–12154.
17. Kruse SW, Zhao R, Smith DP, Jones DN (2003) Structure of a specific alcohol-binding site defined by the odorant binding protein LUSH from Drosophila melanogaster. *Nat Struct Biol* 10(9):694–700.
18. Mascia MP, Trudell JR, Harris RA (2000) Specific binding sites for alcohols and anesthetics on ligand-gated ion channels. *Proc Natl Acad Sci USA* 97(16):9305–9310.
19. Huang CL, Feng S, Hilgemann DW (1998) Direct activation of inward rectifier potassium channels by PIP2 and its stabilization by Gβγ. *Nature* 391(6669):803–806.
20. Zhang H, He C, Yan X, Mirshahi T, Logothetis DE (1999) Activation of inwardly rectifying K^+ channels by distinct PtdIns(4,5)P2 interactions. *Nat Cell Biol* 1(3):183–188.
21. Huang CL, Slesinger PA, Casey PJ, Jan YN, Jan LY (1995) Evidence that direct binding of G protein βγ subunits to the GIRK1 G protein-gated inwardly rectifying K^+ channel is important for channel activation. *Neuron* 15(5):1133–1143.
22. Logothetis DE, Kurachi Y, Galper J, Neer EJ, Clapham DE (1987) The βγ subunits of GTP-binding proteins activate the muscarinic K^+ channel in heart. *Nature* 325(6102):321–326.
23. Reuveny E, et al. (1994) Activation of the cloned muscarinic potassium channel by G protein βγ subunits. *Nature* 370(6485):143–146.
24. Wickman KD, et al. (1994) Recombinant G-protein βγ subunits activate the muscarinic-gated atrial potassium channel. *Nature* 368(6468):255–257.
25. Whorton MR, MacKinnon R (2011) Crystal structure of the mammalian GIRK2 K^+ channel and gating regulation by G proteins, PIP_2, and sodium. *Cell* 147(1):199–208.
26. Kunkel MT, Peralta EG (1995) Identification of domains conferring G protein regulation on inward rectifier potassium channels. *Cell* 83(3):443–449.
27. Rishal I, Porozov Y, Yakubovich D, Varon D, Dascal N (2005) Gβγ-dependent and Gβγ-independent basal activity of G protein-activated K+ channels. *J Biol Chem* 280(17):16685–16694.
28. Finley M, Arrabit C, Fowler C, Suen KF, Slesinger PA (2004) βL-βM loop in the C-terminal domain of G protein-activated inwardly rectifying K^+ channels is important for Gβγ subunit activation. *J Physiol* 555(Pt 3):643–657.
29. He C, Zhang H, Mirshahi T, Logothetis DE (1999) Identification of a potassium channel site that interacts with G protein βγ subunits to mediate agonist-induced signaling. *J Biol Chem* 274(18):12517–12524.
30. Ivanina T, et al. (2003) Mapping the Gβγ-binding sites in GIRK1 and GIRK2 subunits of the G protein-activated K^+ channel. *J Biol Chem* 278(31):29174–29183.
31. Styer AM, et al. (2010) G protein βγ gating confers volatile anesthetic inhibition to Kir3 channels. *J Biol Chem* 285(53):41290–41299.
32. Okamura Y, Murata Y, Iwasaki H (2009) Voltage-sensing phosphatase: Actions and potentials. *J Physiol* 587(Pt 3):513–520.
33. Suh BC, Leal K, Hille B (2010) Modulation of high-voltage activated Ca^{2+} channels by membrane phosphatidylinositol 4,5-bisphosphate. *Neuron* 67(2):224–238.
34. Pegan S, et al. (2005) Cytoplasmic domain structures of Kir2.1 and Kir3.1 show sites for modulating gating and rectification. *Nat Neurosci* 8(3):279–287.
35. Murata Y, Iwasaki H, Sasaki M, Inaba K, Okamura Y (2005) Phosphoinositide phosphatase activity coupled to an intrinsic voltage sensor. *Nature* 435(7046):1239–1243.
36. Blednov YA, Stoffel M, Alva H, Harris RA (2003) A pervasive mechanism for analgesia: Activation of GIRK2 channels. *Proc Natl Acad Sci USA* 100(1):277–282.
37. Howard RJ, et al. (2011) Alcohol-binding sites in distinct brain proteins: The quest for atomic level resolution. *Alcohol Clin Exp Res* 35(9):1561–1573.
38. Benedikt J, Teisinger J, Vyklicky L, Vlachova V (2007) Ethanol inhibits cold-menthol receptor TRPM8 by modulating its interaction with membrane phosphatidylinositol 4,5-bisphosphate. *J Neurochem* 100(1):211–224.
39. Sauguet L, et al. (2013) Structural basis for potentiation by alcohols and anaesthetics in a ligand-gated ion channel. *Nat Commun* 4:1697.
40. Ho IH, Murrell-Lagnado RD (1999) Molecular mechanism for sodium-dependent activation of G protein-gated K^+ channels. *J Physiol* 520(Pt 3):645–651.
41. Inanobe A, Nakagawa A, Matsuura T, Kurachi Y (2010) A structural determinant for the control of PIP_2 sensitivity in G protein-gated inward rectifier K^+ channels. *J Biol Chem* 285(49):38517–38523.
42. Petit-Jacques J, Sui JL, Logothetis DE (1999) Synergistic activation of G protein-gated inwardly rectifying potassium channels by the βγ subunits of G proteins and Na^+ and Mg^{2+} ions. *J Gen Physiol* 114(5):673–684.
43. Sui JL, Chan KW, Logothetis DE (1996) Na^+ activation of the muscarinic K^+ channel by a G-protein-independent mechanism. *J Gen Physiol* 108(5):381–391.
44. Lesage F, et al. (1995) Molecular properties of neuronal G-protein-activated inwardly rectifying K^+ channels. *J Biol Chem* 270(48):28660–28667.
45. Sui JL, Petit-Jacques J, Logothetis DE (1998) Activation of the atrial K_{Ach} channel by the βγ subunits of G proteins or intracellular Na^+ ions depends on the presence of phosphatidylinositol phosphates. *Proc Natl Acad Sci USA* 95(3):1307–1312.
46. Tong W, Sun GY (1996) Effects of ethanol on phosphorylation of lipids in rat synaptic plasma membranes. *Alcohol Clin Exp Res* 20(8):1335–1339.
47. Enkvetchakul D, Jeliazkova I, Bhattacharyya J, Nichols CG (2007) Control of inward rectifier K channel activity by lipid tethering of cytoplasmic domains. *J Gen Physiol* 130(3):329–334.
48. Kobayashi T, Washiyama K, Ikeda K (2004) Inhibition of G protein-activated inwardly rectifying K^+ channels by various antidepressant drugs. *Neuropsychopharmacology* 29(10):1841–1851.
49. Zhou W, Arrabit C, Choe S, Slesinger PA (2001) Mechanism underlying bupivacaine inhibition of G protein-gated inwardly rectifying K^+ channels. *Proc Natl Acad Sci USA* 98(11):6482–6487.
50. Grosman C, Zhou M, Auerbach A (2000) Mapping the conformational wave of acetylcholine receptor channel gating. *Nature* 403(6771):773–776.
51. Whorton MR, MacKinnon R (2013) X-ray structure of the mammalian GIRK2-βγ G-protein complex. *Nature* 498(7453):190–197.